05,06

Modification of the Dispersion Spectrum of Surface Spin Waves in Bilayer YIG Films by a Hybrid Magnonic Crystal

© A.S. Ptashenko, A.V. Sadovnikov

Saratov State University named after N.G. Chernyshevsky
Saratov Russia

E-mail: andrey.po3@mail.ru

Received September 8, 2025
Revised September 8, 2025
Accepted November 12, 2025

In this work, numerical modeling is employed to investigate the physical mechanisms of interaction between surface magnetostatic waves and a conducting medium in a hybrid structure composed of a bilayer iron-yttrium garnet (YIG) film and a metallic magnonic crystal. The study focuses on analyzing the transformation of the dispersion spectrum of surface magnetostatic waves as a function of the metal's electrical conductivity and its spatial position relative to the ferromagnetic layers. The underlying physical mechanism is the excitation of eddy currents in the metallic screen by the time-varying magnetic field of the spin wave. These currents generate a secondary magnetic field that modifies the dipolar field of the wave, thereby altering its dispersion characteristics. It is demonstrated that reducing the metal's conductivity weakens the screening effect, manifesting in the smoothing of anti-crossings between dispersion modes and a narrowing of Bragg bandgaps. A threshold behavior of conductivity is identified: below this threshold, the system behaves virtually as an unshielded bilayer YIG film. The effect is shown to be strongly dependent on the screen's position, which is attributed to the differing spatial overlap between the localized surface magnetostatic wave fields (at opposite interfaces) and the regions of induced eddy currents. These findings contribute to the fundamental understanding of spin-wave electrodynamics in ferromagnet–metal hybrid structures.

Keywords: magnonics; spin waves; hybrid magnonic systems; yttrium iron garnet; magnonic crystal; eddy currents; dipole–dipole interaction; nonreciprocity.

DOI: 10.61011/PSS.2025.11.62974.2k-25

1. Introduction

The study of hybrid magnonic systems, where spin waves interact with the excitations of other physical nature (photons, plasmons, phonons), is one of the key areas in the contemporary physics of magnetism [1,2]. Structures that combine ferromagnetic dielectrics, such as yttrium-iron garnets (YIG), with conducting materials are of special interest. Such a combination makes it possible to study the fundamental aspects of electrodynamic interaction of magnons with conductivity electrons, which opens the prospects of spin-wave process management [3–5].

The relevant area for the studies is the analysis of spin wave propagation and development of a component base, especially for magnonic logical devices [6,7]. Various magnetic structures, such as magnonic crystals, narrow bent waveguides, 2D arrays of magnetic columns or holes in ferromagnetic films, bound waveguides and other unlimited structures, and their edges that may provide for an additional type of excitations [8–10].

Characteristics of spin waves in magnonic structures depend substantially on geometric parameters of waveguides. This is caused, among other factors, by impact of geometric parameters, such as thickness, width and shape, on the value and direction of the internal magnetic field, which in the end impacts the dispersion of spin waves in waveguides [11].

The current trend in CMOS-electronics is expansion from 2D flat to 3D vertically integrated structures. To maintain the same process level, a similar expansion must be implemented in magnonics, which is currently based on planar structures [12].

Three-dimensional (3D) ferromagnetic structures may serve an element base for such devices as microwave filters, interferometers, elements of information transmission and storage etc . [13,14] Use of 3D magnonic structures may also reduce the linear dimensions of developed devices, which in its turn will cause reduction of losses in process of spin wave propagation and, accordingly, reduction of energy losses.

Interaction of a spin wave with metal is of complex nature. The alternating dipole field that accompanies the spin wave penetrates the metal and induces vortex currents there in according to the Faraday's law. These currents create the secondary magnetic field, which counteracts the source field of the wave, effectively screening it. Such inverse exposure causes substantial rearrangement of the disperse spectrum of spin waves: their frequency, group speed change, and additional dissipative decay is introduced (ohmic losses) [15,16].

Use of a periodically structured metal screen (a magnonic crystal) adds an additional physical mechanism — Bragg diffraction of spin waves in periodic heterogeneity [17,18]. As a result, band gaps are formed in the wave spectrum, the

position and width of which depend on both the structure geometry and intensity of the electrodynamic link between the spin wave and metal. Metal electroconductivity at the same time serves as the key parameter that regulates the force of this interaction [19].

This paper studies the physics of magnetostatic surface wave (MSSW) propagation in a complex hybrid system — a two-layer YIG film bound to a metallized magnonic crystal. The two-layer structure as such possesses a rich disperse spectrum including internal and external MSSW modes [20]. The objective of the paper is to establish fundamental patterns of this spectrum transformation under the influence of electroconductivity and geometry of conducting screen location, which will enable deeper understanding of hybridization mechanisms of magnonic and electromagnetic excitations in such structures.

2. Theory

Yttrium-ion garnet ($[Y_3Fe_5O_{12}]$) is a basic material for magnonics due to its unique properties: record low level of losses in spin wave propagation and developed technology of thin film formation [16]. In YIG the spin waves may be described as oscillations of magnetization around the equilibrium direction caused by the external magnetic field.

Spin waves in YIG may be classified as magnetostatic surface waves and body waves. MSSWs are most intereating for practical applications due to their high sensitivity to the interfaces, stability in propagation along the structure and possibility to form band gaps in the spectrum [16].

Maxwell's equations for the structure shown in Figure 1 with appropriate boundary conditions are solved to describe the electrodynamic characteristics. The Floquet periodic boundary conditions (PBC) are specified on the right and left boundaries of the computational domain to ensure calculation of SW dispersion curves for the first reduced Brillouin band, PBC have the following appearance:

$$\vec{E}[C(x+L,y) = \vec{E}(x,y)\exp(-j\beta_y L), \tag{1}$$

where β_y is the component of the wave vector along the axis y (longitudinal wave number).

Numerical simulation and calculation of electromagnetic waves using the finite element method were carried out by solution of the Maxwell system of equations. Besides, the components of the electromagnetic field depend on the frequency according to the harmonic law $e^{j\omega t}$, which allows solving the second-order equation for the electric field strength vector E:

$$\nabla \times (\widehat{\mu}^{-1}\nabla \times E) - k^2\varepsilon E = 0, \tag{2}$$

where $k = \omega/c$ is the wave number in vacuum, $\omega = 2\pi f$ is the circular frequency, f is the frequency of the electromagnetic wave, $\varepsilon = 14$ is the effective dielectric permittivity for the YIG layer.

The magnetic permeability tensor of each layer was specified in the form corresponding to the electromagnetic description of the gyrotropic medium [17]:

$$\widehat{\mu}_{1,2} = \begin{bmatrix} 1 & 0 & 0 \\ 0 & \mu_{1,2}(\omega) & -i\mu_{\alpha 1,2}(\omega) \\ 0 & i\mu_{\alpha 1,2}(\omega) & \mu_{1,2}(\omega) \end{bmatrix}, \tag{3}$$

$$\mu_{1,2}(\omega) = \frac{\omega_H(\omega_H + \omega_{M1,2}) - \omega^2}{\omega_H^2 - \omega^2}, \tag{4}$$

$$\mu_{\alpha 1,2}(\omega) = \frac{\omega_{M1,2}\omega}{\omega_H^2 - \omega^2}, \tag{5}$$

where $\omega_{M1,2} = \gamma 4\pi M_{1,2}$, $\omega_H = \gamma H_0$, $\gamma = 2\pi \cdot 2.8$ MHz/Oe — gyromagnetic ratio in the YIG film, $M_{1,2}$ — saturation magnetization of each layer. For simulation of eigenwave propagation in a periodic structure, it is sufficient to consider one structure period that forms a MC lattice cell.

Formation of the band gaps in the spin wave spectrum is caused by Bragg resonance [18], arising from interaction of waves with the periodic metal strip structure. The width and position of the band gap are defined by the following factors:

Periodic structure parameters: period $L = 200\,\mu$m, metal strip width $w = 100\,\mu$m, to surface $d_h = 1\,\mu$m. Metal screen characteristics: electroconductivity σ, thickness $d_m = 10\,\mu$m. Properties of ferromagnetic layers: saturation magnetization $M_1 = 1738$ Oe, $M_2 = 904$ Oe, thickness of layers $d_1 = 8.9\,\mu$m, $d_2 = 6.9\,\mu$m. The structure is placed into the external magnetic field $H_0 = 670$ Oe, directed perpendicularly to the direction of wave propagation in the XOY plane. Such geometry is chosen on the basis of the fact that the paper studies magnetostatic surface waves (MSSW).

When the specified parameters change, the transformation of spin wave disperse characteristics occurs, which manifests in the shift and change of the band gap width. It is important to note that dielectric permittivity of YIG in numerical simulation is selected a scalar value, magnetic permittivity is described by a tensor depending on frequency, and for simulation it is sufficient to consider one period of the structure that forms a lattice cell of a magnonic crystal.

For the preliminary analysis, an analytical equation was used to find disperse characteristics of the structure [19].

The analytical dispersion equation of MSSW is the following:

$$f^2 = f_H(f_H - f_M) - \frac{f_M^2}{4}\left(1 - e^{-2kxd}\right), \tag{6}$$

where boundary frequencies of the MSSW spectrum:

$$f_{d1,2} = f_H + \frac{f_{M1,2}}{2}, \tag{7}$$

$$f_{p1,2} = \sqrt{f_H(f_H + f_{M1,2})}, \tag{8}$$

$$f_H = \gamma\mu_0 H_0, \tag{9}$$

$$f_{d1,2} = \gamma\mu_0 M_{1,2}. \tag{10}$$

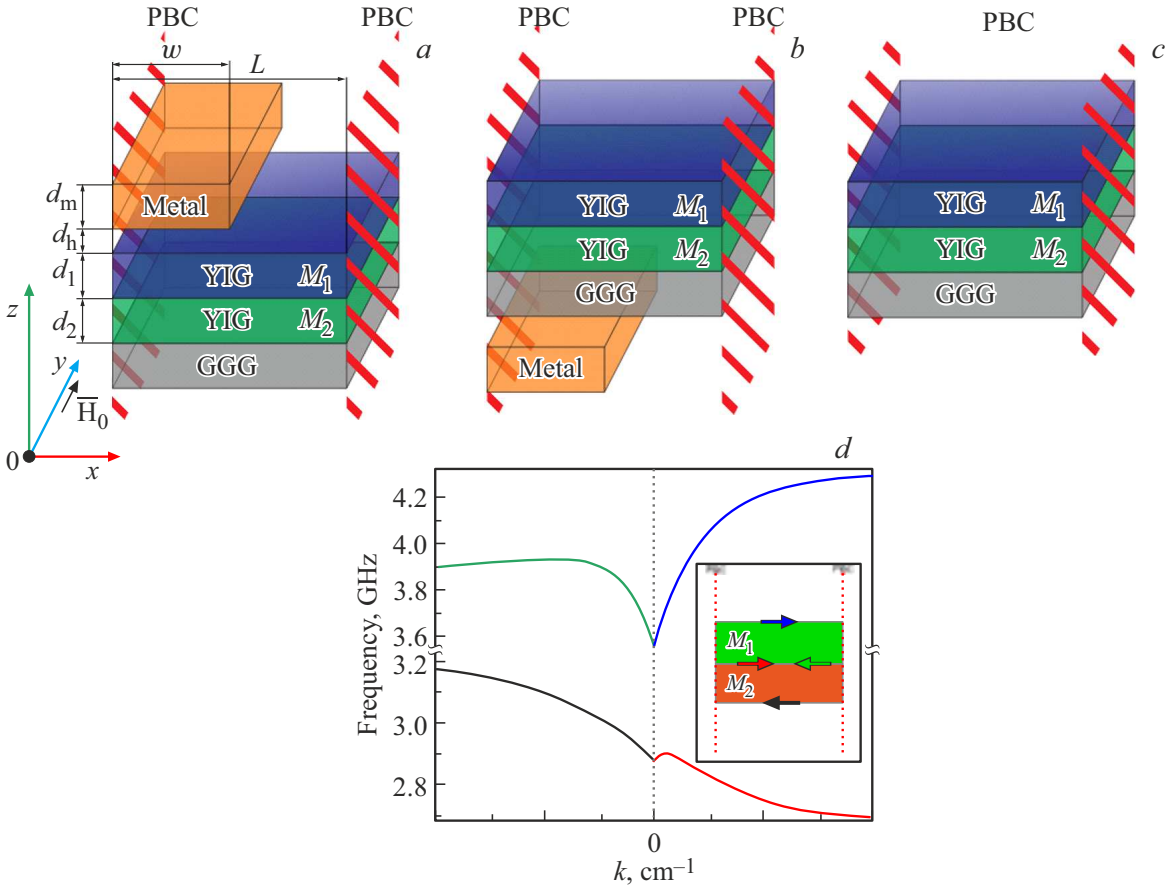

Figure 1. Schematic image of the studied structure with (a) metallization near the layer with magnetization M_1, with (b) metallization near the layer with magnetization M_2, c — fragment of a reference two-layer structure (without metallization), d — disperse characteristic calculated by analytical method for the reference structure of the two-layer film.

In absence of a metal screen, the MSSW spectrum in a two-layer film (Figure 1, d) consists of four branches (for $k > 0$ and $k < 0$). Two of them correspond to „external“ waves localized in the external boundaries of the structure (film-air and film-substrate). Two other ones — to the „external“ waves localized at the interface of two ferromagnetic layers [20]. The presence of two layers with different saturation magnetization results in release of degeneracy and in ability to hybridize these modes, which manifests in the form of anti-crossing (repulsion) of disperse curves.

The approach of the metal screen to the ferrite surface fundamentally changes the boundary conditions for the dipole field of the spin wave. Within the limit of the ideally conducting screen the tangential component of the electric field and normal component of the magnetic field on its surface must be turned to zero. This is equivalent to appearance of a „magnetic image“ and causes considerable increase of the wave number and, accordingly, MSSW frequency [18]. For a metal with the finite conductivity the screening effect decays, and the depth of field penetration into metal is determined by the depth of a skin layer. The periodic structure of the screen causes Bragg's reflection of the wave, which results in occurrence of the band gaps at the borders of the Brillouin zone.

3. Numerical simulation

For the numerical study of the impact of metal screen and magnonic crystal parameters on dispersion characteristics of spin waves, COMSOL Multiphysics software environment was used with an RF Module intended to solve Maxwell's equations in gyrotropic media. The estimated area was broken into an unstructured adaptive grid based on triangular finite elements (finite element method — the method making it possible to solve the Maxwell's equations for a gyrotropic medium with account of the complex geometry of the studied structure). The specific size of the grid element was $0.2\,\mu$m in the ferromagnetic layers of YIG and $0.5\,\mu$m in the field of the metal screen and the surrounding space. Such resolution provides for correct description of both the high-gradient fields near the interface and the skin layer in the metal at maximum conductivity. The check of the convergence results was carried out using a series of test calculations with subsequent decrease of the specific size of elements by 30 % and 50 %. It was established that

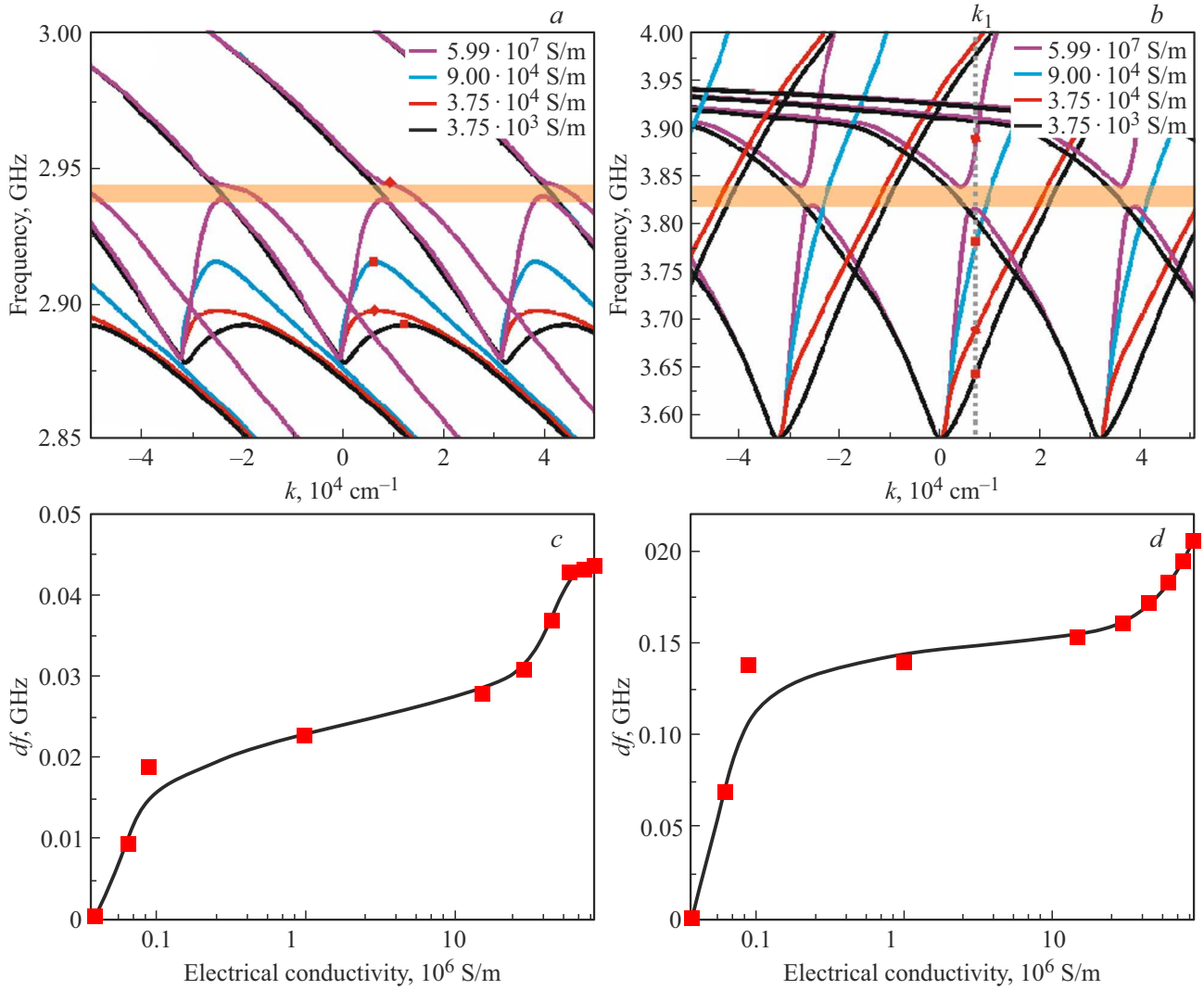

Figure 2. Disperse characteristics for the structure with metallized lattice near the layer with the highest magnetization at different electroconductivity parameters of the metal screen (*a* — low-frequency part of disperse characteristics, *b* — high-frequency part of disperse characteristics), *c* — shift of the maximum value of frequency for the straight wave of disperse characteristics in the LF area in respect to the case without metallization, *d* — frequency shift in HF area with fixed wavelength relative to disperse branches in the structure without metallization.

the change of the resonance frequencies and position of band gaps at the same time does not exceed 1 %, which confirms the sufficient convergence and reliability of the obtained dispersion characteristics.

In contrast to the typical approach to the description of ferromagnetics within the magnetostatic approximation and Walker's equation used for simulation of static or quasistatic magnetic fields with a known type of tensor, electrodynamic performance of MC shall be defined by means of the Maxwell's equation solved for the structure [21] shown in Figure 1, *with* the appropriate boundary conditions.

The completed simulation showed considerable impact of the metal electroconductivity at dispersion characteristics of spin waves.

As you can see in Figure 2, at high conductivity ($\sigma = 5.99 \cdot 10^7$ S/m, which corresponds to copper electroconductivity) a significant spectrum restructuring: considerable shift of dispersion curves to the area of high frequencies and formation of a wide band gap (orange area). Physically it is explained by the strong screening effect of dense vortex currents, which effectively „displace" the magnetic field of the wave from under the metal, which is equivalent to the increase of the effective „hardness" of dipole to dipole interaction and, accordingly, growth of magnon frequency.

As the electroconductivity decreases, the depth of the skin layer increases, the density of induced currents drops, and their screening effect decays. As a result the inverse impact on the spin wave becomes less pronounced, which may be observed in the case when the electroconductivity is accepted to be equal to $9 \cdot 10^5$ S/m, which corresponds to the nickel-chromium parameters. This manifests itself in gradual displacement of dispersion curves back to their

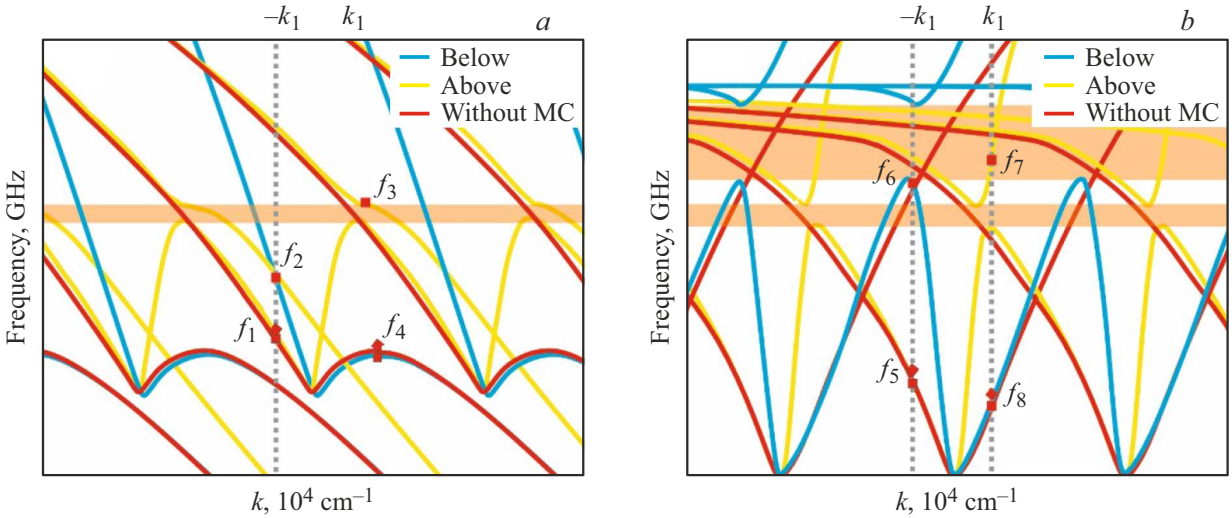

Figure 3. Comparison of disperse characteristics in various positions of magnonic crystal (blue lune — screen at layer with $M_1 = 1738$ Oe, yellow line — in a layer with $M_2 = 904$ Oe) and with its absence (red curve).

position in the unscreened structure and narrowing of the band gap. At $\sigma = 3.75 \cdot 10^4$ S/m, which corresponds to the electroconductivity of alloys with very high resistance (for example, some manganese or chromium alloys), the interaction becomes so weak that the spectrum is practically identical to the case of the film without metal. The conducted analysis made it possible to build the curve of dependence of frequency deviation ($df = f_n - f_{ref}$, where f_n – frequency of the specific points) in the specific points (which are shown in Figure 2, *a, b* with red squares) relative to the values in dispersion branches without a metal screen on the surface. Figure 2, *c* shows a dependence of the maximum frequency value shift for the straight wave of dispersion characteristics in the LF area relative to the case without metallization, and in Figure 2, *d* the shift of frequency in the HF area at the fixed wavelength relative to the dispersion branches in the structure without metallization — qualitatively the nature of the curves is very close, as the electroconductivity value increases, the provided impact increases on the behavior of the propagating spin waves, and deviation of the dispersion branches strengthens relative to the values without metallization, however, this change is of non-linear nature. Besides, a small residual distortion of the branches, especially near the boundary of the Brillouin zone, indicates preservation of a weak disturbing effect of a metal lattice, which in this mode behaves rather as a dielectric one, and not a metal one.

When the screen is located near the layer with the highest magnetization (Figure 1, *a*, the blue line in Figure 3), it most strongly interacts with the high frequency mode of MSSW localized at this boundary. This causes a significant shift of the corresponding branch of the dispersion curve: for example, in the high frequency (HF) area at wave number $k = 3000\,\text{cm}^{-1}$ the frequency increases from $f_8 = 3.65$ GHz (reference case) to $f_7 = 3.88$ GHz, which corresponds to the shift by 230 MHz. At the same time, when the screen is located near the layer with lower magnetization (Figure 1, *b*, the yellow line) the maximum impact is provided on the low frequency (LF) mode: the maximum frequency of the straight wave increases from $f_4 = 2.88$ GHz to $f_3 = 2.95$ GHz, i. e. by 70 MHz.

For the waves with the opposite sign of the wave number ($k < 0$) other shifts are observed, which highlights the nonreciprocal nature of interaction [22]. In particular, in the LF-area at $k = -3000\,\text{cm}^{-1}$ the shift is 30 MHz (from $f_1 = 2.89$ GHz to $f_2 = 2.92$ GHz) with the screen near the layer M_2, whereas with the screen near M_1 the deviation does not exceed 170 MHz (from $f_5 = 3.67$ GHz and to $f_6 = 3.84$ GHz).

Therefore, the position of the screen makes it possible to selectively reinforce or suppress the interaction with the specific MSSW modes, which is the direct effect of the various spatial localization of their dipole fields. This selectivity manifests both in the value of the frequency shift and in the extent of nonreciprocity reinforcement, and may be used for mode filtering and control of the direction of spin signal propagation.

4. Conclusion

This paper studied theoretically the electrodynamic interaction of magnetostatic waves with a hybrid magnonic crystal formed by a two-layer film of yttrium-iron garnet and a periodically structured metal screen. The paper demonstrated selective modulation of the dispersion spectrum due to the change in the spatial position of the periodic screen relative to the layers with different magnetization. It is shown that the external and internal MSSW modes respond differently to the presence of the screen, which opens the possibility of mode selection in the hybrid magnonic systems. A threshold nature of dependence of dispersion

characteristics on the metal electroconductivity is found: at $\sigma \lesssim 10^5$ S/m the screen impact becomes negligibly low, and the spectrum practically matches the case of the non-screened film. It is established that the simultaneous effect of Bragg diffraction and vortex current screening causes a complex transformation of mode anti-crossing that may not be described in the single-layer models.

It should be noted that in the real heterogeneity structures — such as roughness of boundaries, variations of layer thickness or periodicity defects — may cause additional scattering of spin waves and erosion of band gaps [23–25]. However, in this paper we are focused on the idealized model making it possible to detect the key physical mechanisms of hybridization of magnonic and electromagnetic excitations. The analysis of the impact of structural and process defects is planned in the subsequent papers.

Therefore, the produced results expand the understanding of hybridization mechanisms of magnonic and electromagnetic excitations in multi-layer ferrite-metal structures and open new possibilities for design of the magnonic devices with the controlled selectivity and nonreciprocity.

Funding

This study was supported financially by the Russian Science Foundation, grant No. 23-79-30027.

Conflict of interest

The authors declare that they have no conflict of interest.

References

[1] A. Barman, G. Gubbiotti, S. Ladak, A.O. Adeyeye, M. Krawczyk, J. Gräfe, C. Adelmann, S. Cotofana, A. Naeemi, V.I. Vasyuchka, B. Hillebrands. J. Phys.: Condens Matter, **33**, *41*, 413001 (2021).
[2] B. Flebus, D. Grundler, B. Rana, Y. Otani, I. Barsukov, A. Barman, G. Gubbiotti, P. Landeros, J. Åkerman, U. Ebels, P. Pirro. J. Phys.: Condens Matter, **36**, 363501 (2024).
[3] P.A. Popov, A.Y. Sharaevskaya, E.N. Beginin, A.V. Sadovnikov, A.I. Stognij, D.V. Kalyabin, S.A. Nikitov. J. Magn. Magn. Mater. **476**, 423 (2019).
[4] A.K. Zvezdin, A.S. Logginov, G.A. Meshkov, A.P. Pyatakov. Bull. Russ. Acad. Sci.: Phys. **71**, 1561 (2007).
[5] S. Sugahara, J. Nitta. Proc. IEEE **98**, *12*, 2124 (2010).
[6] P.G. Baranov, A.M. Kalashnikova, V.I. Kozub, V.L. Korenev, Y.G. Kusrayev, R.V. Pisarev, V.F. Sapega, I.Y. Akimov, M. Bayer, A.V. Scherbakov, D.R. Yakovlev. Phys. Usp. **62**, *8*, 795 (2019).
[7] Y. Chai, Y. Liang, C. Xiao, Y. Wang, B. Li, D. Jiang, P. Pal, Y. Tang, H. Chen, Y. Zhang, H. Bai. Nat. Commun. **15**, *1*, 5975 (2024).
[8] W. Namiki, Y. Yamaguchi, D. Nishioka, T. Tsuchiya, K. Terabe. Mater. Today Phys. **45**, 101465 (2024).
[9] V.V. Tikhonov, A.S. Ptashenko, A.V. Sadovnikov. J. Phys. D: Appl. Phys. **58**, *7*, 07LT01 (2024).
[10] S.A. Odintsov, S.E. Sheshukova, S.A. Nikitov, A.V. Sadovnikov. Phys. Rev. Appl. **22**, *1*, 014042 (2024).
[11] H.T. Nguyen, T.M. Nguyen, M.G. Cottam. Phys. Rev. B **76**, *13*, 134413 (2007).
[12] D. Sander, S.O. Valenzuela, D. Makarov, C.H. Marrows, E.E. Fullerton, P. Fischer, J. McCord, P. Vavassori, S. Mangin, P. Pirro, B. Hillebrands. J. Phys. D: Appl. Phys. **50**, *36*, 363001 (2017).
[13] A.V. Chumak, P. Kabos, M. Wu, C. Abert, C. Adelmann, A.O. Adeyeye, J. Åkerman, F.G. Aliev, A. Anane, A. Awad, C.H. Back. IEEE Trans. Magn. **58**, *6*, 1 (2022).
[14] E.N. Beginin, A.V. Sadovnikov, A.Y. Sharaevskaya, A.I. Stognij, S.A. Nikitov. Appl. Phys. Lett. **112**, *12*, 122401 (2018).
[15] A.S. Ptashenko, S.A. Odintsov, S.E. Sheshukova, A.V. Sadovnikov. FTT **66**, *6*, 789 (2024). (in Russian).
[16] A.A. Serga, A.V. Chumak, B. Hillebrands. J. Phys. D: Appl. Phys. **43**, *26*, 264002 (2010).
[17] S.A. Nikitov, P. Tailhades, C.S. Tsai. J. Magn. Magn. Mater. **236**, *3*, 320 (2001).
[18] E.N. Beginin, Y.A. Filimonov, E.S. Pavlov, S.L. Vysotskii, S.A. Nikitov. Appl. Phys. Lett. **100**, *25*, 252501 (2012).
[19] S.A. Odintsov, S.E. Sheshukova, S.A. Nikitov, E.H. Lock, E.N. Beginin, A.V. Sadovnikov. J. Magn. Magn. Mater. **546**, 168736 (2022).
[20] V.I. Zubkov, B.P. Nam. ZhTF **59**, *12*, 115 (1989). (in Russian).
[21] D.D. Stancil, A. Prabhakar. Spin Waves. Vol. 5. New York: Springer, 2009.
[22] S.A. Odnintsov, E.G. Lokk, E.N. Beginin, A.V. Sadovnikov, Russ. Technol. J. **10**, *4*, 55 (2022).
[23] A.V. Chumak, A.A. Serga, S. Wolff, B. Hillebrands, M.P. Kostylev. J. Appl. Phys. **105**, *8*, 083903 (2009).
[24] M.A. Abeed, S. Sahoo, D. Winters, A. Barman, S. Bandyopadhyay. Sci. Rep. **9**, *1*, 16635 (2019).
[25] K. Di, V.L. Zhang, M.H. Kuok, H.S. Lim, S.C. Ng, K. Narayanapillai, H. Yang. Phys. Rev. B **90**, *6*, 060405 (2014).

Translated by M.Verenikina